


Article

Enhanced Retention and Synergistic Plugging Effect of Multi-Complexed Gel on Water-Swellable Rubber

Tong Li ¹, Wenwu Yang ², Jiajun Wu ³ , Peidong Xing ³, Qian Xu ³, Hegao Liu ³ and Guangsheng Cao ^{3,*}¹ School of Petroleum Engineering, Northeast Petroleum University, Daqing 163318, China² Exploration and Development Research Institute, Daqing Oilfield Co., Ltd., Daqing 163000, China³ Key Laboratory of Enhanced Oil & Gas Recovery of Ministry of Education, Northeast Petroleum University, Daqing 163318, China

* Correspondence: nepucgswz@163.com

Abstract: For the management of fractured large pores in high-water-bearing reservoirs, the general approach is to use transfer dissection and sealing. Conventional regulators have a limited regulating radius and can only produce blocking in the near-well zone, which is not ideal. Deep dissection technology can expand the radius of action and substantially improve the blocking effect. The existing deep-dissection agent system has problems such as high cost and poor effect, which affect its large-scale application. In this paper, to address these problems, a gel-type dissection modifier cross-linking agent was synthesized and optimized in the laboratory using low-concentration polymer, and the factors affecting the final gel formation effect were experimentally studied. The final polymer concentration was chosen to be 1500 mg/L~3000 mg/L, the poly-crossing ratio was 30:1, the pH was controlled at 7–9, and the temperature was controlled at 30–60 °C; the rubber was formed with good shear resistance and thermal stability, and had good adaptability to the high-mineralization environment. The optimal injection concentration of water-expanded rubber particles for this system was confirmed to be 3000 mg/L. Cryo-electron microscopy was used to observe the morphology of polymer gel formation and the adhesion of nucleated water-expanded particles to the gel, to clarify the mechanism of enhanced retention and sealing of nucleated water-expanded rubber particles by the multiple complex gel system, and finally to verify the sealing performance of the composite sealing system and determine the use effect by indoor simulation experiments with a two-dimensional flat plate model. This study is of great significance for the efficient development of high-water-bearing late reservoirs and further improvement of crude oil recovery.

Keywords: high-water cut reservoir; high-permeability fractured channels; compound profile control agent system; plugging mechanism



Citation: Li, T.; Yang, W.; Wu, J.; Xing, P.; Xu, Q.; Liu, H.; Cao, G. Enhanced Retention and Synergistic Plugging Effect of Multi-Complexed Gel on Water-Swellable Rubber. *Energies* **2022**, *15*, 8096. <https://doi.org/10.3390/en15218096>

Academic Editors: Ali Habibi, Jan Vinogradov and Zhengyuan Luo

Received: 3 October 2022

Accepted: 26 October 2022

Published: 31 October 2022

Publisher's Note: MDPI stays neutral with regard to jurisdictional claims in published maps and institutional affiliations.



Copyright: © 2022 by the authors. Licensee MDPI, Basel, Switzerland. This article is an open access article distributed under the terms and conditions of the Creative Commons Attribution (CC BY) license (<https://creativecommons.org/licenses/by/4.0/>).

1. Introduction

After initial short-term natural energy self-injection production in the oil field, most crude oil is produced by polymer injection to provide displacement power. When the oil-field enters the development period of high-water cut or ultra-high-water cut, the utilization rate of polymer injection is low and the cycle of inefficiency and ineffectiveness is serious. In order to control the inefficient and ineffective circulation and improve the development effect, the method of profile control is mainly used to block the dominant seepage channel of water flow in the oil layer, thereby changing the direction of liquid flow in the oil layer. Large-hole channel control technology has a history of nearly 30 years [1]. Since the 1990s, Williamson [2] and others have summarized the large-hole channel-plugging technology. Xiao [3] studied the pore structure change characteristics of sandstone reservoirs with high porosity and high permeability after water flooding. Chuan [4] summarized the variation characteristics and variation mechanism of reservoir physical properties in the process of reservoir development. Zheng [5] found that reservoirs with high permeability, coarse grain

size and good physical properties are more prone to high-permeability regions. Zhang [6] studied the gel properties of acrylamide polymer under chromium crosslinking to improve the stability of chromium in solution, and applied it to the treatment of large pores. Mack J C [7] used over-crosslinked polymer to treat large pores near the wellbore, and successfully applied this treatment method to cased wells and open hole completions, reducing the production well water output. Nikolov A [8] deduced the identification criteria of large pores and applied them through the characteristics of high-speed non-Darcy seepage in large pores and the seepage identification criteria. At this stage, the method of blocking high-permeability channels is mainly used to control large pores, and local profile control and plugging in the interval is the main treatment method for blocking high-permeability channels. The types of profile control agents that are used the most are: granular profile control agents, gel profile control agents, flocculation profile control agents, polymer microsphere profile control agents, resin profile control agents, foam profile control agents. Polymer based profile control agents are the most commonly used technology for treating large pore channels. The commonly used polymer profile control agents can be roughly divided into low- and medium-molecular-weight polymers and high-molecular-weight polymers according to their material composition and structure. According to their properties, they can be divided into anionic, cationic and nonionic polymers [9]. With the further increase of water cut in old oilfields, plugging control technology has been developed from a single oil water well to large-scale overall plugging control. In recent years, with the gradual deepening of oilfield development, the contradiction between injection and production has further deepened, and various new profile control and water plugging technologies have been developed, such as plugging control technologies for vertical wells, deep wells, horizontal wells, ultra-deep wells, and high-temperature wells [10]. The 2D physical model of microscopic glass etching is used to study the plugging control mechanism. At the same time, research on deep-profile control technology has not stopped, and a variety of deep profile control agents have been developed, such as colloidal dispersion gel (CDG) and weak gel deep profile control agent [11]. Throughout China's deep-profile control technology, composite ionic polymer profile control technology, polyacrylamide/chromium ion gel technology, xanthan gum/chromium ion gel technology, delayed cross-linking technology, colloidal dispersion gel technology, pre-crosslinked bulk granules and other deep profile control technologies are mainly used [12].

The development of water plugging and profile control technology abroad has gone through roughly six stages [13]. In the early 20th century, cement plugging agents were mainly used. In the 1950s, heavy oil, water in oil emulsion and oil well cement were mainly used as water blocking agents. From the 1960s to the 1970s, polyacrylamide polymer gel water blocking agents were widely used. In the late 1980s, people developed water glass profile control agents and granular profile control agents. In the early 1990s, for special working conditions, various deep profile control systems such as weak gels, ultra-micro-bacteria, surfactants and microorganisms were applied on site and achieved certain results. At present, the most widely used deep profile control agents in foreign countries include weak gel deep profile control systems and delayed cross-linking gel systems, which are represented by the colloidal dispersion gel series of Tiorco Company in the United States and Marathon in the United States [14]. The polymer-Cr³⁺ gel series and the profile control-water blocking agent series are produced by the Phillip Petroleum Company of the United States [15].

Polymer weak gel technology is an emerging water-controlling and oil-increasing technology. Its flood control mechanism is that the nano-scale/micron-scale polymer microspheres flow with the dominant water flow channels such as medium- and high-permeability layers with low injection pressure through hydration. Expansion and adsorption results in accumulation plugging or bridging plugging in formation pore throats, slowly cross-linking under reservoir temperature conditions to form a gel with a certain strength, thus producing resistance to subsequent water injection and increasing the water injection sweep range [16]. The microspheres will elastically deform under a certain

pressure, thus breaking through the pore throat and continuing to migrate to the deep formation. Weak gel is a low-concentration polymer and cross-linking agent mainly based on intermolecular cross-linking and supplemented by intra-molecular cross-linking, thereby forming a cross-linked body with a three dimensional network structure. It is called “flow gel” or “movable gel” [17]. First, the weak gel system not only has high strength, but also can block high-permeability layers in the formation. Secondly, due to the weak cross-linking strength of the weak gel, the weak gel will gradually transfer to the deep part of the formation under the continuous promotion of injected water, resulting in oil displacement [18]. At present, weak gels at home and abroad mainly include metal complexes (such as aluminum citrate, chromium acetate, etc.) and organic molecules (phenolic resin, N'-methylenebisacrylamide, etc.), polyacrylamide or xanthan gum. They are prepared with cross-linking agents such as aluminum citrate, chromium acetate, glyoxal and phenolic resin prepolymer [19]. The advantage of the weak gel deep profile control system is that it has strong selectivity, good shear resistance and can migrate in the formation. Permanent damage has no effect on later measures. The disadvantage is that the cross-linking time is short, which leads to a sharp increase in the subsequent injection pressure. The dilution of formation water and the adsorption loss of cross-linking agents will affect the weak gel system in the formation. The gelling state and the system is also not resistant to salt and high temperature [20].

On the basis of the previous research, this paper studies a new complex gel system in the laboratory by using low-concentration polymers for the weak retention capacity of coreless water-swelling rubber, and synthesizes the gel-type profile control according to the synthesis principle. The formulation was optimized and the factors affecting the final gelation effect were experimentally studied. The gel morphology of the polymer after gelation was observed by cryo-electron microscopy, and the adhesion between the coreless water-swelling particles and the gel was clear. The multi-component complex gel system strengthens the retention and blocking mechanism of nucleated water-swelling rubber particles. Finally, through the indoor simulation experiment of the two dimensional flat plate model, the blocking performance of the composite plugging system is verified and the use effect is determined.

2. Experimental Part

2.1. Experimental Materials

The experimental equipment is shown in Table 1.

Table 1. Experimental equipment and instruments.

Serial	Device Name	Specifications	Test Range	Test Accuracy
1	Electric incubator	HH-W21-600	37.0~150.0 °C	±1.0 °C
2	Water bath	BX-101	25.0~95.0 °C	±1.0 °C
3	Hand pump	CY-1	0.0~30.0 MPa	±0.1 MPa
4	High-pressure metering pump	JB-III	0.0~50.0 MPa	±0.01 MPa
5	Electronic balance	JA5003	0.0~500.0 g	±0.001 g
6	TA rheometer	TA2000EX		
7	Low speed mixer	JJ-1		

Experimental compounds include cross-linking agents: lactic acid, acetic acid, propionic acid, malonic acid, oxalic acid, tartaric acid and malic acid. High-priced metal compounding agents are: potassium dichromate, chromium trichloride, zirconium oxychloride, titanium tetrachloride, aluminum trichloride, aluminum citrate and ethylene glycol. Initiators are: thiourea, sodium thiosulfate, sodium nitrite, ammonium chloride, anhydrous sodium sulfite, polyacrylamide, etc.

2.2. Synthesis of Multi-Component Complex Gel Cross-Linking Agent

Experimental principle: The multi-complexed gel profile control agent is mainly composed of polyacrylamide, high-efficiency cross-linking agent, and alkaline control agent. Under the initiation of the basic control agent, polyaddition, cross-linking and other polymerization reactions occur to form a glue, and a high-strength polymer with a network structure is formed. The reaction principle is shown in Figure 1.

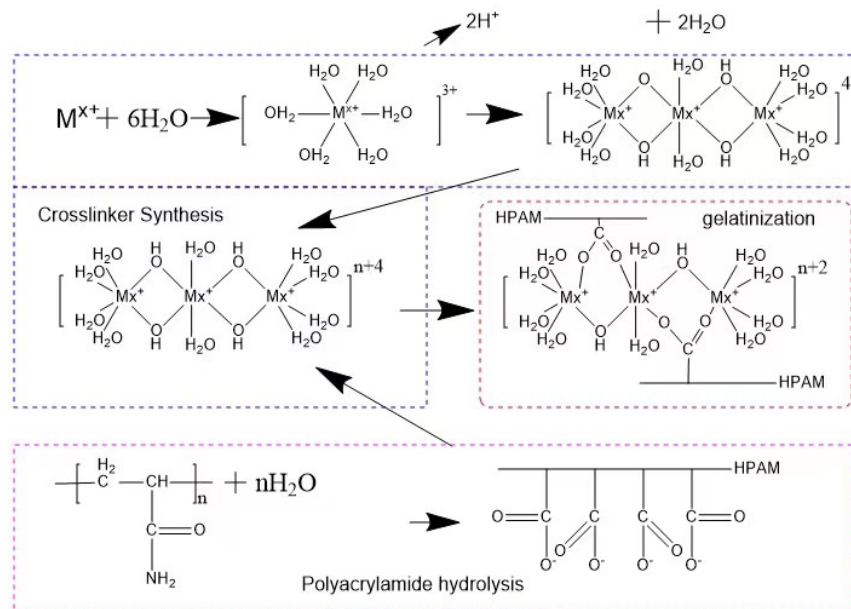


Figure 1. Schematic diagram of cross-linking reaction.

Experimental scheme: The content of dimers, trimers and linear trimers (Figure 2) is controlled by optimizing the ratio of reactants, the pH value of the system, and the optimization of compounding agents, by adding activators, further increase The higher active linear trimer content in the system can improve the reactivity of the cross-linking agent and enhance the strength of the network structure jelly formed with $-COO^-$ in HPAM, by adding a small amount of complex aluminum salt, through the secondary cross-linking It can inhibit the water loss and shrinkage of the gel, and further improve the stability of the gel system.

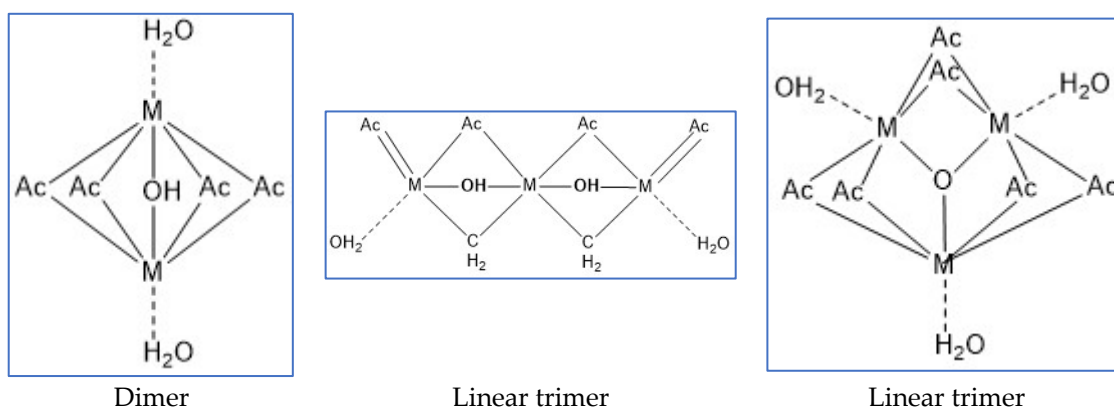


Figure 2. Synthetic product structure diagram.

Lactic acid, malonic acid, propionic acid, citric acid, oxalic acid, tartaric acid, malic acid, etc. are all good organic complexing agents. The complex acid is subjected to cross-linking reaction to prepare the cross-linking agent system.

Experimental steps: (1) Add 100 mL of water to a four-necked flask with a condensation reflux device. (2) Add 1 g of high-value metals into water and stir for 10 minutes. (3) Slowly add complexing agent and regulator, and stir for 10 min respectively. (4) Slowly add 0.2% complexing agent and regulator and stir for 10 min. (5) Heat to 50–90 °C until the reaction is completed. (6) After the synthesis of the cross-linking agent, the synthesized cross-linking agent is obtained after aging in an oven at 45 °C for 24 hours. (7) Record the experimental conditions and experimental phenomena. After the cross-linking agent is prepared, make it gel with the polymer solution, and study the factors affecting the gel forming effect.

2.3. Synergistic Plugging Experiment of Multi-Complexed Gel and Water Swellable Rubber

2.3.1. Research on Plugging Rate and Erosion Resistance

Experimental scheme: The experiment uses a self-made core model, changes the size of the fractures and pores in the core model by changing the overlying rock pressure (6 Mpa, 8 Mpa, 10 Mpa, 12 Mpa and 14 Mpa) and tests the multi-complexed gel and water swellable rubber particles for plugging performance of cracked large pores after combined use. The injected particle size is 0.150–0.250 mm, 0.250–0.420 mm; the concentration is 3000 mg/L water-swelling rubber particles and 2000 mg/L polymer solution.

Experimental steps: (1) Inject the working solution of the cross-linking agent with a polymer cross ratio of 30:1 at a speed of 2 mL/min. (2) After 7 days of holding, inject water into the formation to measure the breakthrough pressure and stable pressure. (3) Calculate the residual resistance coefficient and plugging rate, and then water drive the core by 5.0 PV. (4) Check the plugging performance and scour resistance of the two profile control agents combined, and observe the outlet end of the core.

2.3.2. Study on the Influence of Residual Oil Distribution in Fractured Channels

Experimental scheme: The cemented flat core is used as the experimental object in the experiment, and the experimental device is composed of a core simulation system, a data acquisition system and a pressure control system, to study the fluid migration law and the remaining oil distribution law in large fractured pores. The flowchart is shown in Figure 3.

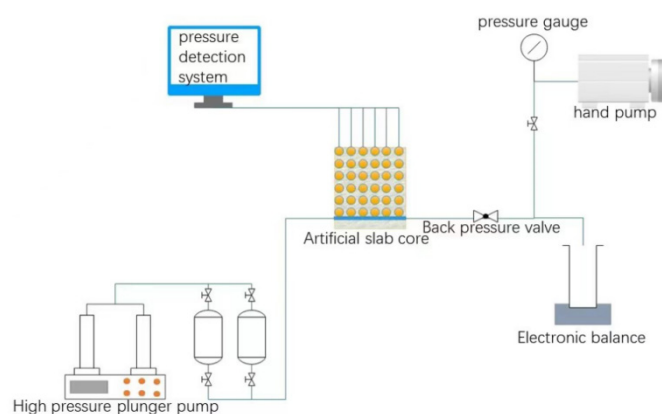


Figure 3. Schematic diagram of flat core experiment.

The flat cores are prepared through the steps of material mixing, quartz sand filling, cement configuration, model forming and curing and cementation. The model permeability can be controlled by adjusting the quartz sand particle size and auxiliary content, the porosity can be controlled by the cement content, and the porosity can be controlled by adding clay minerals and natural core debris were used to simulate the pore structure of the core. Fractures were artificially created in the center of the flat core and 36 pressure-measuring points of 6×6 were set at the same interval on one side of the fracture to measure the pressure change.

Experimental steps: (1) After checking the air tightness of the flat core, vacuum the flat core at multiple points through the reserved pressure-measuring holes to make the flat model reach a complete vacuum; then, connect the fluid tank through the reserved non-vacuuming point to saturate the flat core. After the water is saturated with oil, the experimental device is assembled to carry out the experiment. (2) First, water flooding was performed from the inlet of the artificial fracture at a rate of 0.5 ml/min until the water content reached 95%; then, the water flooding was stopped and the core pressure changes at different times were recorded according to the number of injected PVs. (3) The water-swellable rubber particles, the multi-complex gel cross-linking agent and the polymer solution were injected into the flat core model at a rate of 0.5 mL/min for a total of 0.2 PV, and the gel was completely formed after 7 days of coagulation. (4) Carry out water flooding at a rate of 0.5 mL/min, stop the experiment when the water content reaches 98%, and record the core pressure changes at different times according to the injection amount.

2.3.3. Evaluation of Water Cut and Recovery Factor

Experimental scheme: The experiment used a self-made core model. The size of the cracks in the core model was changed by changing the pressure of the overlying rock. The pressure of the overlying core was set to 8 MPa, particles with a particle size range of 0.250–0.420 were injected and water-swellable rubber was injected. The particle concentrations were 1000 mg/L, 2000 mg/L, 3000 mg/L and 4000 mg/L, respectively, to test the effect of water-swellable particle concentration on water content and recovery factor after the combination of multi-complex gel and water-swellable rubber particles.

Experimental steps: (1) Vacuum the core to saturate it with water and then saturate it with oil, and then drive the core to a water content of 98% to measure the water drive pressure. (2) Inject 0.2 PV of 3000 mg/L water-swellable rubber particle polymer solution with different concentrations at a rate of 1 mL/min, and inject formation water after stabilization to measure the stable pressure of water flooding. (3) Draw the curve of water content and recovery factor under different particle concentrations.

3. Results and Discussions

3.1. Influencing Factors of Multi-Complex Gel System Gelation

The gel-forming performance was evaluated in the clear water system and the sewage system; the pH of the gel-forming environment was set to 6–8 and the temperature was 45 °C.

It can be seen from Table 2 that the polymer concentration of this system in clean water and sewage can be formed into glue from 500–3000 mg/L; the glue-forming time is 1–5 days and the glue-forming viscosity is greater than 3800 mPa·s when using water for solution. The viscosity of the glue formed when using the sewage solution is slightly lower than that of the clean water system, which shows that it has strong adaptability to water quality and can be formed into a glue in a high-salinity environment. The polymer concentration is an important factor affecting the performance of the profile control agent. The polymer–cross ratio is 20:1 and the pH value is 8.5. Figure 4a shows the curves of gelling time and strength versus polymer concentration. In addition to polymer concentration, the polymer–cross ratio is another factor that affects the gelling time and viscosity. The polymer concentration is 1500 mg/L, and the pH value is 8.5. The curves of gelling time and viscosity versus polymer–cross ratio are shown in Figure 4b.

With the increase of polymer concentration, the gelling time is shortened and the gelling viscosity is increased. Based on the comprehensive consideration of gelling time, gelling viscosity and cost, the optimal polymer concentration is 1500–3000 mg/L. With the increase of the polymer–cross ratio, the gelling time increases and the gelling viscosity decreases. Through the comprehensive consideration of the gelling time, gelling viscosity, and cost, the polymer to cross ratio of 30:1 was selected as the amount of cross-linking agent for profile control agent. The influence of different pH values on the gelling strength

and gelling time of the system was checked to determine the applicable pH range. The experimental results are shown in Table 3.

Table 2. Effects of concentration and polymer-to-cross ratio on gel formation.

Polymer Concentration (mg/L)	Aggregate Cross Ratio	Gel Time (d)	Branch Water		Produced Water	
			Initial Viscosity (mPa·s)	Gel Viscosity (mPa·s)	Initial Viscosity (mPa·s)	Gel Viscosity (mPa·s)
500	20:1–40:1	1–5	11	3800	6.8	3600
1000	20:1–40:1	1–5	37	8000	16.2	5200
1500	30:1–40:1	1–5	92	20,000	31	8900
2000	30:1–40:1	1–5	151	22,000	50	14,000

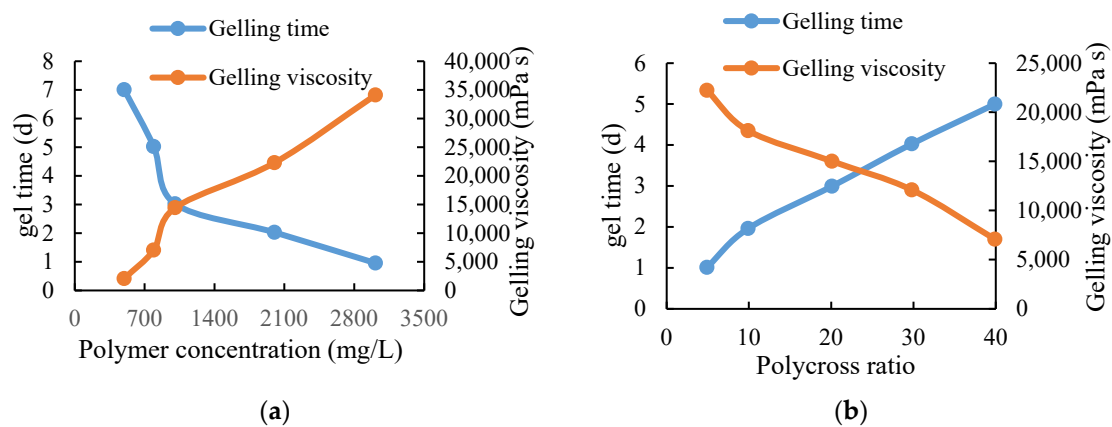


Figure 4. Polymer gelling performance curve. (a) The relationship curve of polymer concentration, gel time and gel viscosity. (b) The relationship curve of poly-cross ratio, gel time and gel viscosity.

Table 3. The effect of pH on gel formation.

Number	pH	Polymer Concentration (mg/L)	Aggregate Cross Ratio	Gelling Time (d)	Gelling Viscosity (mPa·s)
1	6	2000	30:1	/	/
2	7	2000	30:1	7	9000
3	8	2000	30:1	4	13,400
4	9	2000	30:1	3	14,500
5	10	2000	30:1	1	12,000

With the gradual increase of pH value, the gelling time is gradually shortened, but with the increase of pH value to a certain extent, the gelling viscosity will also decrease, so a pH value between 8–9 is the best. In order to test the stability of the multi-component complex gel system under alkaline conditions, 0.1–0.3% weak base surfactant was mixed into the system solution [21]; the results are shown in Table 4.

Table 4. Multi-complex type and ternary system compatibility system experiment.

Polymer Concentration (mg/L)	Gelling Environment (pH)	Surfactant Concentration (%)	Gelling Time (d)	Gelling Viscosity (mPa·s)
1500	8~9	0.1~0.3	1~3	7500
3000	8~9	0.1~0.3	1~3	16,000

It can be seen that the multi-component complex gel system can still form gel in the presence of surfactant, indicating that the gel is less destructive and more stable under

alkaline conditions. Considering the influence of mechanical shearing on the system performance, the solution was sheared for 60 seconds at 6000 rpm [22]. See Table 5 for the experimental results.

Table 5. The effect of shear on the performance of the system.

Number	Polymer Concentration (mg/L)	Cutting Mode	Initial Viscosity (mPa·s)	Viscosity after Shearing (mPa·s)	Gelling Time (d)	Gelling Viscosity (mPa·s)
1	1500	Uncut	135	Uncut	4	8900
2	1500	Shear	132	93	4.5	6800
3	2000	Uncut	222	Uncut	3	11,900
4	2000	Shear	219	131	3	10,800
5	3000	Uncut	354	Uncut	2	21,900
6	3000	Shear	349	211	2.5	20,700

The indoor mechanical shearing has no obvious effect on the gel system. Although the initial viscosity of the solution after shearing is greatly reduced, the system after shearing can still be gelled, and the viscosity and transaction time do not change much. Place the gelled sample in an oven at 45 °C, and measure the viscosity change of the system at regular intervals. See Table 6 for the experimental results.

Table 6. Thermal stability evaluation results.

Polymer Concentration (mg/L)	Aggregate Cross Ratio	Viscosity under Different Conditions (mPa·s)					
		Initial Gelling	10 d	30 d	60 d	90 d	120 d
500	30:1	1000	3600	3560	3480	3410	3350
1000	30:1	1000	5200	5150	5070	4990	4920
1500	30:1	8900	8850	8800	8600	8350	8200
2000	30:1	12,000	11,900	11,700	11,400	11,100	10,800
3000	30:1	22,400	22,300	22,100	21,900	21,200	20,400

It can be seen that the system has good thermal stability. After 4 months of storage, the viscosity changes little and the viscosity loss rate is within 10%. Through the above experiments, the performance of the developed cross-linking agent system was evaluated and the best formulation of the cross-linking agent system was preliminarily screened. See Table 7 for the system performance evaluation results.

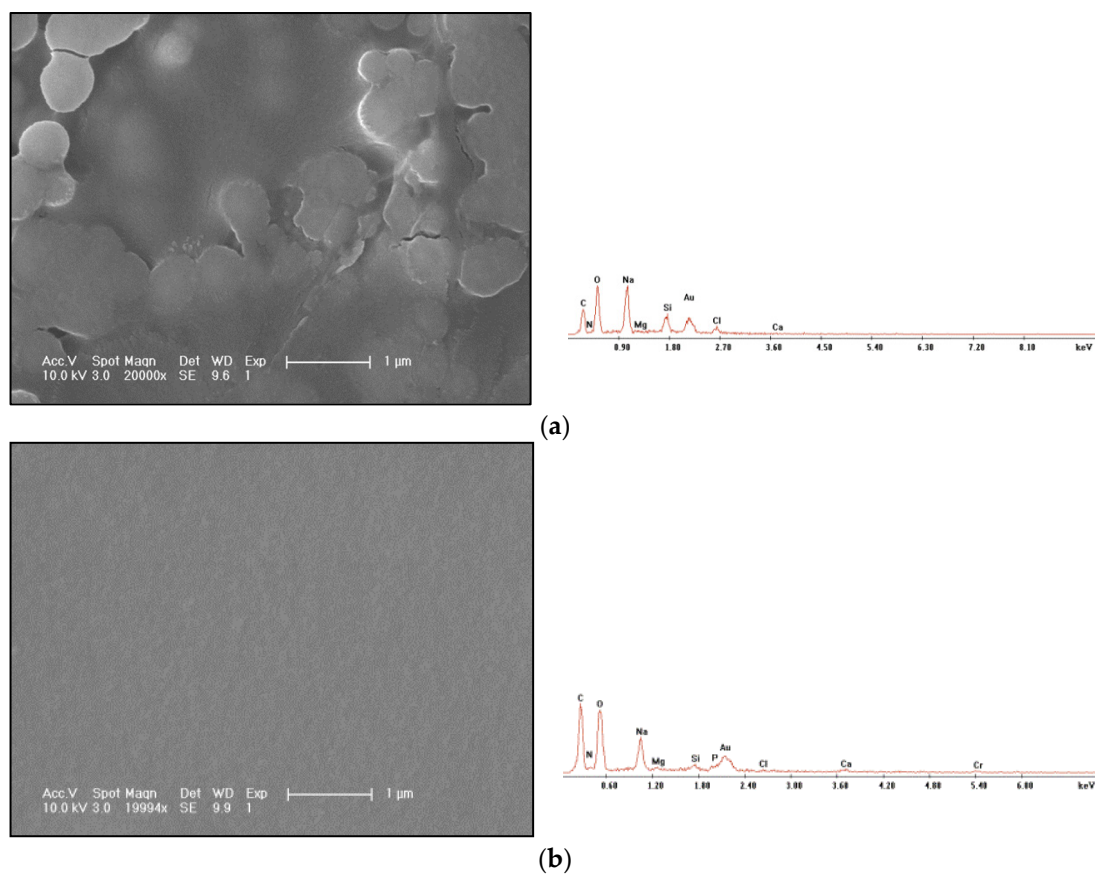
Based on the requirements of gelling time and viscosity, the polymer concentration can be selected between 1500 mg/L and 3000 mg/L, the polymerization cross ratio is 30:1, the pH value is between 7–9, and the temperature is between 30 °C and 60 °C. After gelling, the appearance is dark green, the gelling time and viscosity are good, and it has good shear resistance and thermal stability. It has good adaptability to the environment with high salinity.

3.2. Study on Enhanced Retention Mechanism

The morphology observation and energy spectrum characterization of polyacrylamide freeze-drying are shown in Figure 5a, and the morphology observation and energy spectrum characterization of gel freeze-drying are shown in Figure 5b.

Table 7. Crosslinking agent performance evaluation test result table.

Polymer Concentration (mg/L)	Aggregate Cross Ratio	Initial Viscosity (mPa·s)	Gelling Time (d)	Gelling Viscosity (mPa·s)	pH	Effective Content (%)	Applicable Temperature (°C)
500	30:1	10	5d	2685	7–9	2–4	30–60
1000	30:1	93	4d	5836			
1500	30:1	135	4d	9037			
2000	30:1	249	3d	12,770			
2500	30:1	309	2d	22,390			
3000	30:1	339	2d	22,640			

**Figure 5.** Freeze-drying SEM photos and EDS energy spectrum. (a) Polyacrylamide solution. (b) Polyacrylamide chromium gel.

Through comparison, it can be found that the film-forming integrity of the polymer is obviously worse than that of the gel, and the film surface breaks, indicating that the film forming strength and density of the polymer are very low. After freeze-drying, the structure is loose, the overall structure is easy to damage and the shear resistance is poor. The gel obviously has the properties of forming a compact membrane and spatial network structure, which is the reason why the gel can be mechanically retained in the core channel.

The changes of the gel at different time in the gelling process were analyzed, and the SEM morphology and EDS characterization were compared. The gel morphology observation and energy spectrum characterization of the original sample are shown in Figure 6a; the gel morphology observation and energy spectrum characterization of 0.150–0.250 mm after the gel is placed for a period of time are shown in Figure 6b; the gel morphology observation and energy spectrum characterization of 0.250–0.420 mm are shown in Figure 6c.

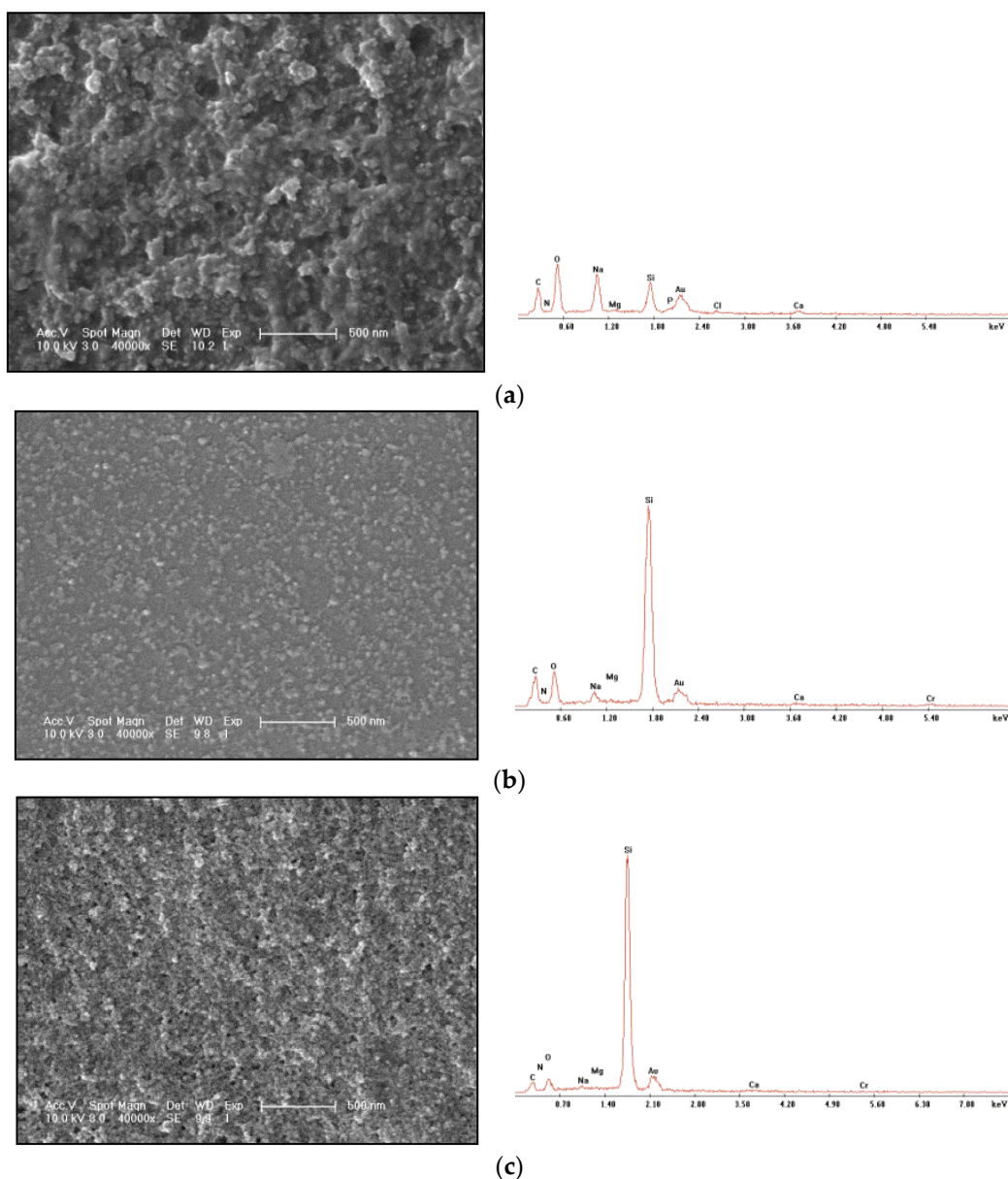


Figure 6. Changes at different times during gel formation. (a) Gel freeze-drying SEM photos and EDS energy spectrum of the original sample. (b) SEM photos and EDS energy spectrum of 0.150–0.250 mm gel freeze-drying. (c) SEM photos and EDS spectra of 0.250–0.420 mm gel freeze-drying.

It can be seen from the comparison that the particle diameter of the original sample gel is larger than that of the 0.250–0.420 mm gel. From the energy spectrum, it can be seen that the original sample of the gel with large particles does not show the energy spectrum signal of Cr^{3+} , which indicates that Cr^{3+} is seriously wrapped by the large polymer particle gel. The space network structure can be seen from 0.150–0.250 mm gel. The formation of this space network structure should be that the polymer first gelatinizes into granular gel; then, the gel particles continue to cross-link through Cr^{3+} . It can be seen from the 0.250–0.420 mm gel that the gel forms a uniform and stable membrane on the silicon wafer surface. Although the 0.150–0.250 mm gel also forms a uniform membrane, the 0.150–0.250 mm gel contains a large amount of granular gel. It can be seen that the Cr^{3+} encapsulated in the gel will gradually cross-link with the granular gel in the polymer to form a network spatial structure. With time, this structure will become more uniform and stable without a large number of granular gels. The gel morphology of the unconsolidated cores is shown in Figure 7.

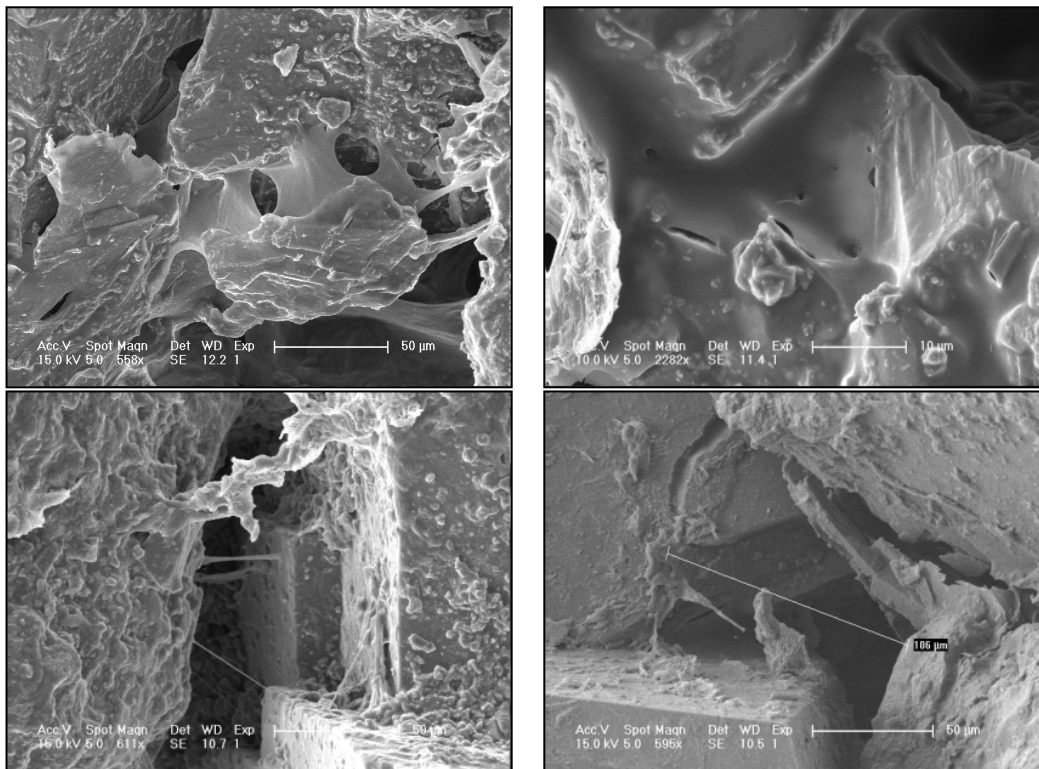


Figure 7. The gel morphology of unconsolidated cores.

According to the core SEM photos, the pore size of the core is generally 30–100 μm range. When the gel is in the freeze-drying state, the water in the gel is removed under the sublimation condition, so the original morphology of the gel can be kept to the maximum extent. For example, under the condition of saturated adsorbed water, these gels will fill the pores and play the role of plugging. Further observation found that the membrane was damaged and had holes due to electron bombardment, which fully proved that the membrane was an organic membrane. The gel morphology of long core after waiting for solidification is shown in Figure 8.

It can be seen that after 7 days of waiting for setting, the surface of the core obviously presents the film shape characteristics of gel, and the core pores are full of gel. Wire mesh gel between core pores. The gelling state is obviously better than that of non-waiting core. It can be seen from the comparison of morphology and gelling ability that the polymer in the continuous migration state does not easily form gel. To sum up, the multi-component complexing gel can enter the deep formation and form a network structure gel with the polymer to seal the formation. The strength of this gel is higher than that of the polymer gel, and the gel-forming effect after waiting is obviously higher than that of the non-waiting gel. This structure can not only seal the formation, but also work with the particle-type profile control agent to improve the sealing effect and erosion resistance.

3.3. Research on Collaborative Plugging Mechanism

For cores with different permeability, the core-plugging performance was tested, and the erosion resistance of cores with multi-component complexing gel and particles of different sizes was tested, as shown in Table 8.

It can be found that the permeability of the core after combined use of multi-component complexing gel and water-swelling rubber particles is decreased after washing, but the permeability is decreased less than that of the single-injected particles, and the plugging rate remains at a high level [23]. From the observation of the outflow particles at the outlet end, it can be seen that the particles injected with water-swelling particles alone flow out more, and a large number of particles can also be seen in the drainage fluid. Compared

with the core outlet end and the outflow fluid washed after the combination of the two, the particles are obviously much less, which proves that a large number of particles are retained in the core. The rubber particles are blocked and wrapped by the gel through the bridging function, so that the particles do not easily flow out with the liquid flow. In addition, the gel can also play the role of a plug, plugging the pores that the particles cannot enter, playing a better plugging effect. In order to verify this statement, experiments were carried out on the influence of multi-component complex gel and water-swelling rubber particles on the distribution of the remaining oil in high-water cut fracture-type large channels. The measurement results are shown in Figure 9.

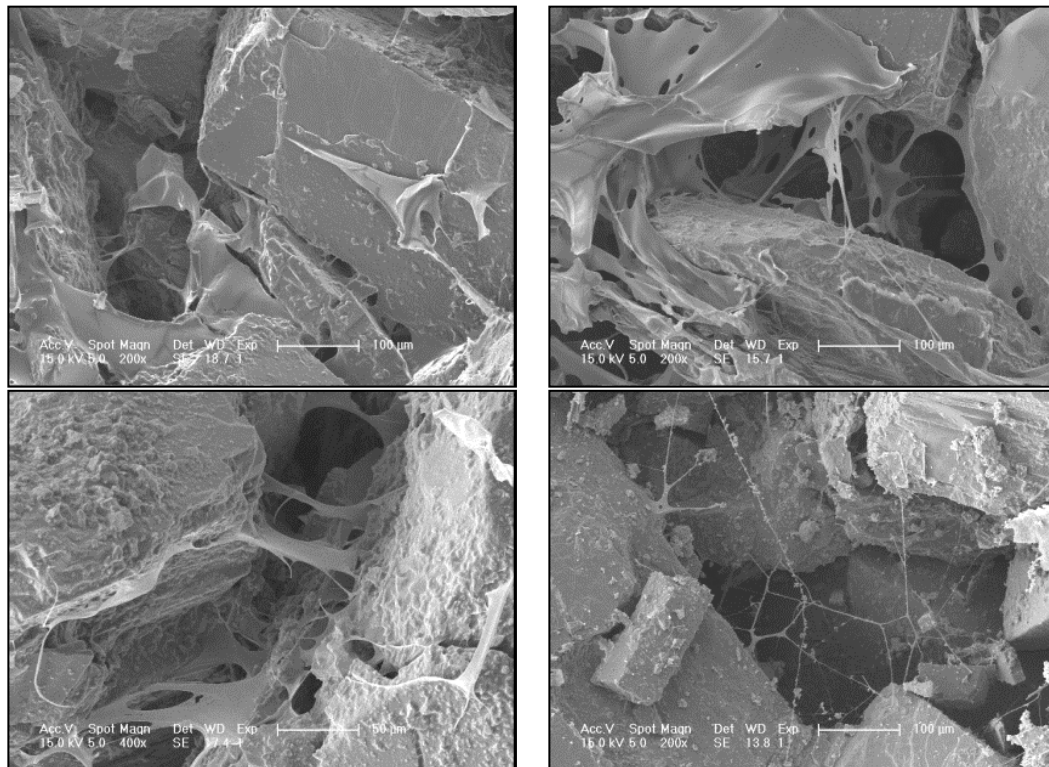


Figure 8. Morphological characteristics of gel of long core after waiting for solidification.

Table 8. Final plugging rate of synergistic system under different overlying rock pressures.

Core Number	Particle Size (mm)	Overburden Rock Pressure (MPa)	Pressure after Plugging (MPa)	Plugging Rate	Pressure after Scouring (MPa)	Final Plugging Rate
1	0.150–0.250	6	0.039	96.92%	0.012	89.77%
		8	0.115	97.83%	0.028	91.06%
		10	0.165	96.42%	0.075	92.15%
		12	1.757	99.63%	0.154	95.77%
		14	1.852	98.65%	0.572	95.63%
2	0.250–0.420	6	0.080	98.26%	0.022	93.49%
		8	0.195	98.67%	0.050	94.79%
		10	1.786	99.72%	0.146	96.58%
		12	1.523	99.56%	0.316	97.88%
		14	0.528	95.55%	0.371	93.67%

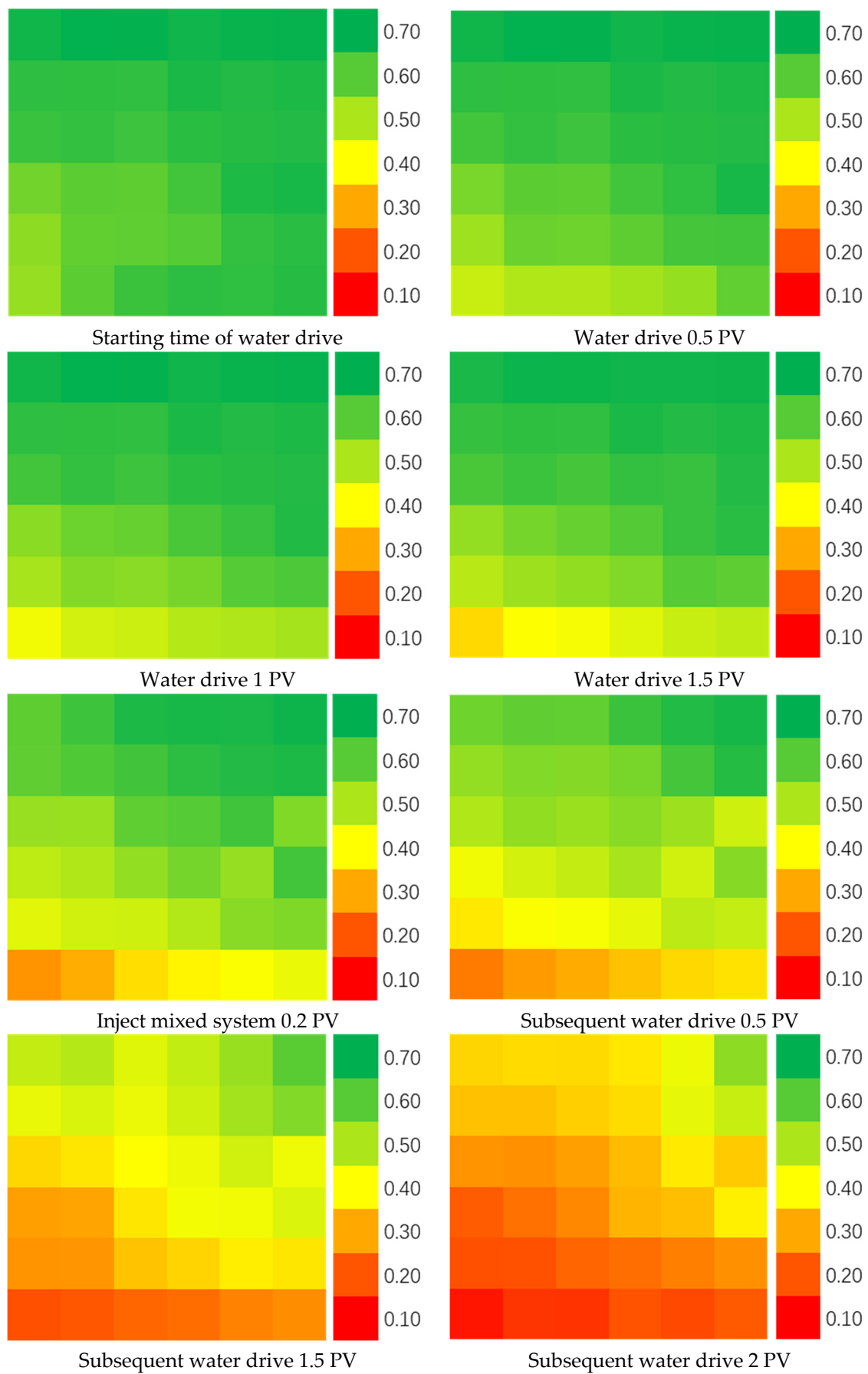


Figure 9. Oil saturation distribution.

It can be seen that after water flooding, the liquid flows out with the high-permeability fracture channel and has difficulty entering the low-permeability area. There is still a large amount of remaining oil that has not been displaced and remains in the core. After the water-swelling rubber particles and gels are injected into the core, not only the overall oil saturation is decreased, but the oil saturation in the low-permeability area that was difficult to reach before decreases significantly as well, which indicates that after the treatment, while the remaining oil in the high-permeability area is further driven out, the liquid body also enters the low-permeability area to bring out the remaining oil in the pores and the treatment has achieved good results. The water cut and recovery curves of fractured macropore cores under different particle concentrations are shown in Figure 10.

From the change curve of the water cut, it can be seen that the water cut in the water drive will increase earlier with the increase of particle concentration in different rubber particle concentrations. It can be seen from the recovery curve that the recovery efficiency of rubber particles with the concentration of 1000 mg/L and 2000 mg/L differs greatly from that of rubber particles with the concentration of 3000 mg/L and 4000 mg/L. Although the recovery efficiency of rubber particles with the concentration of 3000 mg/L is low at the beginning of water flooding, the injection volume increases. Finally, the recovery efficiency of rubber particles with the concentration of 4000 mg/L is similar to that of rubber particles with the concentration of 4000 mg/L. Considering the cost, 3000 mg/L water-swelling rubber particles should be selected for operation.

To sum up, the polymer in the original fracture-sealing system is combined with the multi-component complex gel cross-linking agent to stabilize the water-swelling rubber particles in the fractures, so that it can strengthen the retention capacity of the non-nuclear water-swelling rubber particles while plugging the fractures. In addition, the polymer system can enter the smaller pores near the fractures, achieve the plugging of the scour zone and low-saturation oil area, and greatly enhance the plugging effect.

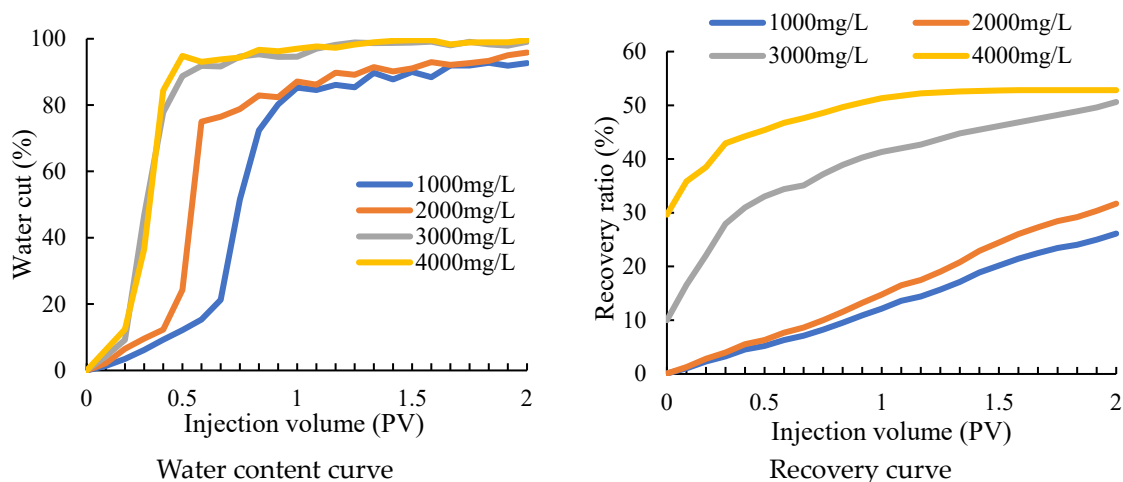


Figure 10. Variation curve of water cut and recovery factor under different concentrations.

4. Conclusions

- (1). In view of the disadvantage of water-swelling rubber not being resistant to erosion, a multiple-complex polymer gel was developed to enhance the plugging effect. The multi-component complex gel crosslinker was synthesized and its specific application range was determined; polymer concentration was 1500 mg/L~3000 mg/L, polymer cross ratio was 30:1, pH value was 7–9 and temperature was 30–60 °C.
- (2). The enhanced retention mechanism of the multi-component complexing gel and water-swelling rubber results from the Cr^{3+} encapsulated in the gel gradually cross-linking with the granular gel in the polymer to form a reticular spatial structure. As time goes on, this structure will become more and more uniform and stable without a

large number of granular gels, and the gelling effect after waiting is obviously higher than that without waiting. Therefore, this structure can completely play the role of sealing the formation.

- (3). It is confirmed that the plugging performance of the combination of water-swelling rubber particles and multi-component complex polymer gel is better than that of the single injection of particles, and the erosion resistance is improved. The oil displacement ability of this system was further confirmed by the saturated oil experiment of with flat core. Through the water content and oil recovery experiments, it was confirmed that the optimal injection concentration of water-swelling rubber particles in this system is 3000 mg/L.

Author Contributions: Conceptualization, T.L.; methodology, W.Y.; writing—original draft preparation, J.W.; validation, P.X.; resources, Q.X.; data curation, H.L.; software, G.C. All authors have read and agreed to the published version of the manuscript.

Funding: This research received no external funding.

Data Availability Statement: Not applicable.

Conflicts of Interest: The authors declare no conflict of interest.

References

1. Xie, K.; Cao, W.; Lu, X.; Song, K.; Liu, Y.; Zhang, Y.; Liu, J.; Lv, J.; Wang, W.; Na, R. Influence of water dilution on performance of chromium polymer weak gel in porous medium. *J. Dispers. Sci. Technol.* **2020**, *41*, 1549–1558. [[CrossRef](#)]
2. Williamson Nathan, H.; Dower April, M.; Codd Sarah, L.; Broadbent Amber, L.; Gross, D.; Seymour Joseph, D. Glass Dynamics and Domain Size in a Solvent-Polymer Weak Gel Measured by Multidimensional Magnetic Resonance Relaxometry and Diffusometry. *Phys. Rev. B Condens. Matter Mater. Phys.* **2019**, *122*, 068001. [[CrossRef](#)] [[PubMed](#)]
3. Xiao, L.; Lin, W.; Xiao, H.; Yong, X. Factors Influencing Viscosity of Twin-Tail Hydrophobically Associating Polymer Weak Gel. *Appl. Mech. Mater.* **2014**, *3436*, 98–101.
4. Chuan, Z. Identification and quantitative description of large pore path in unconsolidated sandstone reservoir during the ultra-high water-cut stage. *J. Pet. Sci. Eng.* **2014**, *122*, 10–17. [[CrossRef](#)]
5. Zheng, X.; Liu, M. Discussion on inverse lotion polymerization process of polyacrylamide. *J. Putian Univ.* **2014**, *7*, 68–71.
6. Zhang, L.; Pu, C.; Yang, J. Application of graft copolymer of ultra-fine cellulose and acrylamide in profile control and water plugging. *Oilfield Chem.* **2015**, *32*, 503–506.
7. Mack, J.C.; Smith, J.E. In depth colloidal dispersion gels improve oil recovery efficiency. *J. Geosci. Res. Northeast. Asia* **2000**, *2*, 207–209.
8. Zhang, H.; Nikolov, A.; Wasan, D. Enhanced oil recovery (EOR) using nanoparticle dispersions: Underlying mechanism and imbibition experiments. *Energy Fuels* **2014**, *28*, 3002–3009. [[CrossRef](#)]
9. Behrens, E.J. Investigation of Loss of Surfactants during Enhanced Oil Recovery Applications Adsorption of Surfactants onto Clay Materials. Master's Thesis, Norwegian University of Science and Technology, Trondheim, Norway, 2013.
10. Yu, S.; Guangsheng, C.; Tianyue, G.; Zhe, L.; Yujie, B.; Dan, L.; Zihang, Z. Development of gelled acid system in high-temperature carbonate reservoirs. *J. Pet. Sci. Eng.* **2022**, *216*, 110836.
11. Abu-Abdeen, M.; Elamer, I. Mechanical and swelling properties of thermoplastic elastomer blends. *Mater. Des.* **2010**, *31*, 808–815. [[CrossRef](#)]
12. Choi, S.S.; Ha, S.H. Water swelling behaviors of silica-reinforced NBR composites in deionized water and salt solution. *J. Ind. Eng. Chem.* **2010**, *16*, 238–242. [[CrossRef](#)]
13. Snoeck, D.; Jensen, O.M.; Belie, N.D. The influence of superabsorbent polymers on the autogenous shrinkage properties of cement pastes with supplementary cementitious materials. *Cem. Concr. Res.* **2015**, *74*, 59–67. [[CrossRef](#)]
14. Dehbari, N.; Tang, Y. Water swellable rubber composites: An update review from preparation to properties. *J. Appl. Polym. Sci.* **2015**, *132*, 42786–42797. [[CrossRef](#)]
15. Zhang, Z.; Zhang, G.; Wang, C. Chlorohydrin water-swelling rubber compatibilized by an amphiphilic graft copolymer.III.Effects of PEG and PSA on water-swelling behavior. *J. Appl. Polym. Sci.* **2015**, *79*, 2509–2516. [[CrossRef](#)]
16. Jia, H.; Ren, Q. Evidence of the gelation acceleration mechanism of HPAM gel with ammonium salt at ultralow temperature by SEM study. *SPE Prod. Oper.* **2016**, *31*, 238–246. [[CrossRef](#)]
17. Xiao, Y.; Tao, Y.; Zhuhua, Z. Fly Ash-based Geopolymers: Effect of Slag Addition on Efflorescence. *J. Wuhan Univ. Technol. (Mater. Sci.)* **2016**, *31*, 689–694.
18. Naghizadeh, A.; Ekolu, S.O. Method for comprehensive mix design of fly ash geopolymer mortars. *Constr. Build. Mater.* **2019**, *202*, 704–717. [[CrossRef](#)]

19. Assi, L.N.; Deaver, E.; ElBatanouny, M.K. Investigation of early compressive strength of fly ash-based geopolymer concrete. *Constr. Build. Mater.* **2016**, *112*, 807–815. [[CrossRef](#)]
20. Zhao, J.; Zhang, J.; Xiang, W.T. Distribution and presence state of polymer in porous media. *J. China Univ. Pet.* **2013**, *37*, 109–113.
21. Wu, B.; Ma, X.; Zheng, Z. Weathering properties of alkali activated slag fly ash cementitious materials. *Nonmet. Miner.* **2020**, *43*, 6–10.
22. Yu, S.; Guangsheng, C.; Tianyue, G.; Zihang, Z.; Yujie, B.; Jiajun, W.; Liming, Y. Evaluation of deep penetration of high-temperature sustained-release acid based on the reaction kinetics and conductivity of acid-etched fractures. *Case Stud. Therm. Eng.* **2022**, *38*, 102336.
23. Lu, Z.J.; Lautru, J.; Zemb, T.; Rebiscoul, D. Colloidal sol of UO₂ nanoparticles supported by multi-lamellar vesicles of carboxylate based surfactant. *Colloids Surf. A Physicochem. Eng. Asp.* **2020**, *10*, 125207. [[CrossRef](#)]